IOP Publishing | Institute of Physics and Engineering in Medicine Physiological Measurement
Physiol. Meas. **00** (2017) 1–13 UNCORRECTED PROOF

Fractal analysis of heart rate variability reveals alterations of the integrative autonomic control of circulation in paraplegic individuals

Paolo Castiglioni[1] **and Giampiero Merati**[1,2]

[1] IRCCS Fondazione Don C Gnocchi, Milan, Italy
[2] Department of Biomedical Sciences for Health, Università degli Studi di Milano, Milan 20133, Italy

E-mail: pcastiglioni@dongnocchi.it

Received 28 September 2016, revised 5 January 2017
Accepted for publication 23 January 2017
Published

Abstract

The autonomic nervous system plays a major role in the integrative control of circulation, possibly contributing to the 'complex' dynamics responsible for fractal components in heart rate variability. Aim of this study is to evaluate whether an altered autonomic integrative control is identified by fractal analysis of heart rate variability. We enrolled 14 spinal cord injured individuals with complete lesion between the 5th and 11th thoracic vertebra (SCI_H), 14 with complete lesion between 12th thoracic and 5th lumbar vertebra (SCI_L), and 34 able-bodied controls (AB). These paraplegic subjects have an altered autonomic integrative regulation, but intact autonomic cardiac control and, as to SCI_L individuals, intact autonomic splanchnic control. Power spectral and fractal analysis (temporal spectrum of scale coefficients) were performed on 10 min tachograms. AB and SCI_L power spectra were similar, while the SCI_L fractal spectrum had higher coefficients between 12 and 48 s. SCI_H individuals had lower power than controls at 0.1 Hz; their fractal spectrum was morphologically different, diverging from that of controls at the largest scales (120 s). Therefore, when the lesion compromises the autonomic control of lower districts, fractal analysis reveals alterations undetected by power spectral analysis of heart rate variability.

Keywords: detrended fluctuation analysis, heart rate variability, autonomic nervous system, spinal cord lesion

(Some figures may appear in colour only in the online journal)

JNL:PMEA PIPS: AA5B7E TYPE: SPE TS: NEWGEN DATE:1/2/17 EDITOR: IOP SPELLING: US

1. Introduction

Since the first report of Kobayashi and Musha in the 80's (Kobayashi and Musha 1982), a large number of studies showed the presence of self-similar, or fractal, components in the beat-by-beat series of heart rate (Huikuri *et al* 2009, Perkiomaki 2011, Sassi *et al* 2015). A time series is self-similar if it shows scale invariance, which means that a short segment looks like the whole series, at least in statistical terms, if the axes of time and amplitude are properly rescaled. This property makes a segment extracted from a time series similar to a fragment cut out from a geometric fractal.

Self-similar time series are typically generated by complex systems that converge into a dynamical state not characterized by an intrinsic time scale (Bak *et al* 1987). Typically, complex dynamical systems have a geometrical fractal structure that connects a large number of individual components interacting each other. The cardiovascular system can be considered such a complex system, because it is composed by a fractal network of branching tubes (West *et al* 1997) that connects several vascular beds regulated locally to provide the blood flow requested at any time by the corresponding body district in response to demands varying over time. However, local regulatory mechanisms are hierarchically coordinated at higher levels to preserve homeostasis and to allow the cardiovascular system responding to external stimuli or to changes in activity levels. We may expect that this 'complex' regulation is not characterized by an intrinsic time scale and that it is responsible for the fractal components often reported in heart-rate variability signals.

The sympathetic and parasympathetic branches of the autonomic nervous system play a major role in the integrative coordination of local regulatory mechanisms. On one hand, the autonomic nervous system transmits information on cardiocirculatory variables (like blood pressure in arteries, blood volumes in the cardiac chambers and in the pulmonary circulation, as well as data on blood chemical composition) to the higher centres of the nervous system. On the other hand, its efferent outflows modify heart rate, stroke volume or the hydraulic resistance of individual vascular beds, transmitting commands from the central nervous system. A large body of literature demonstrated the capability of traditional spectral methods of heart rate variability to quantify changes in the cardiac sympatho/vagal balance that follow changes in the cardiac sympathetic tone or in the cardiac vagal tone (Task Force of the European Society of Cardiology and the North American Society of Pacing and Electrophysiology 1996). However, given the above premises, it may be hypothesized that alterations in the integrative mechanisms responsible for the overall cardiovascular regulation affect specific aspects of heart-rate self similarity more directly and substantially than they may affect traditional heart-rate spectral powers. Thus, fractal analysis of heart rate variability could be more effective than power spectral analysis in revealing alterations of the overall autonomic integrative control of circulation, particularly when the autonomic control of heart rate is not directly affected.

Aim of the present study is to evaluate whether fractal and spectral analysis of heart rate variability identify an altered autonomic integrative control. This is done by assessing power spectra and fractal spectra of scale coefficients in controls and in individuals with a spinal cord lesion between the fifth thoracic vertebra, T5, and the fourth lumbar vertebra, L4. In fact, these spinal cord injured individuals represent a model of altered autonomic regulation for the vascular districts innervated by the pelvic nerves and by sympathetic pathways that leave the medulla below the lesion level, while the vagal and sympathetic innervations of the heart, and the feedback loop of the cardiac baroreflex, are intact. In particular, to also evaluate the effects of the lesion level on fractal and power spectra of heart rate variability, the study considers

two groups of spinal cord injured individuals separately: those with a level of the spinal lesion sufficiently high to also affect the autonomic regulation of the vascular splanchnic districts and those with a lower lesion level, that guarantees an intact splanchnic autonomic regulation.

2. Methods

2.1. Ethical approval

The study was approved by the Ethics Committee of our institution. Each subject gave informed consent prior to the start of the experimental procedure.

2.2. Participants and data collection

Data were collected among paraplegic individuals consecutively seen in our center of Sports Medicine to receive a medical certificate for sports activities (wheelchair basketball, fencing, or swimming), and in a group of healthy volunteers. Paraplegic participants usually trained two-three times weekly, with one session devoted to increase aerobic performance and/or strength and the others to develop technical skills. All paraplegic individuals with a complete traumatic spinal cord lesion (ASIA scale A) with level between T5 and L4 were eligible for this study. Each paraplegic subject underwent a clinical examination, during which anthropometric data and the level of the spinal lesion were recorded. Subjects with current or previous history of overt dysautonomia, including episodes of syncope, fainting, hypotension, reflex tachycardia in the last 6 months, were excluded. In eligible subjects, the ECG was recorded for 10 min, with sampling rate of 200 Hz. All subjects were studied several hours after any significant physical activity, to avoid possible carry-over effects of acute fatigue on heart-rate variability. Recordings were obtained in a quite environment, in sitting position, after an adaptation period at rest of at least 5 min. Subjects were asked to breath spontaneously during the recording without speaking.

A total of 37 spinal-cord injured (SCI) individuals with lesion between T5 and L4 were considered eligible for the study. Fourteen of them (2 females and 12 males, age 40.9 + 10.0 years, body mass index 25.5 + 4.8 kg m^{-2}, mean + SD) had a lesion level between T12 and L4. These SCI individuals compose the sub-group with the low-level lesion (SCI_L). Among the remaining subjects, with lesion level between T5 and T11, we selected 14 individuals similar to the low-level group in terms of age (37.1 + 6.6 years), body mass index (24.6 + 4.1 kg m^{-2}) and gender composition (1 female and 13 males). These individuals compose the subgroup with the high-level lesion (SCI_H). Figure 1 illustrates the extension of expected impairment in the integrative autonomic control for these two SCI groups.

From our database of ECG recordings in healthy individuals, we selected 34 subjects with age (39.3 + 12.1 years), body mass index (24.7 + 2.6 kg m^{-2}) and gender composition (5 females and 29 males) similar to the two SCI_L and SCI_H subgroups. These able-bodied subjects compose the control group (AB). ECG recordings were obtained in AB subjects with the same experimental protocol followed for recording ECG in SCI_L and SCI_H individuals. Two participants of the SCI_H group and three of the SCI_L group were taking antibiotics for urinary tract infections; two in the SCI_H group and two in the SCI_L group were taking oral bacoflen to relieve muscle spasms.

The beat-by-beat series of *R–R* intervals were derived from the ECG after parabolic interpolation of the *R*-wave maximum. Premature beats were identified visually and removed before power spectral analysis and fractal analysis.

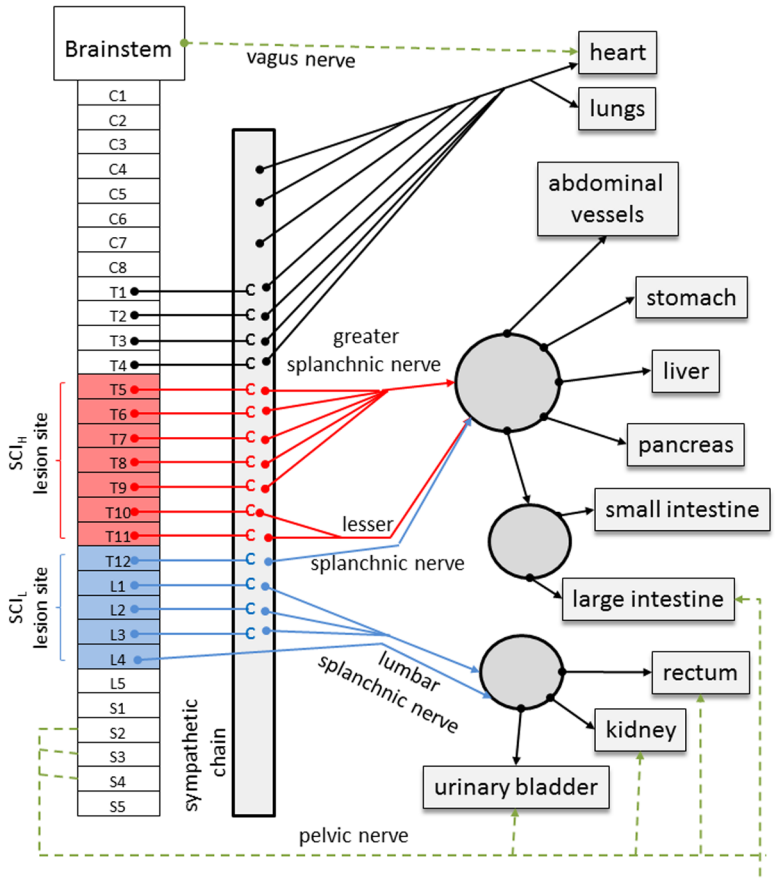

AQ5

Figure 1. Simplified scheme of autonomic efferent pathways relevant for illustrating SCI_L and SCI_H human models of altered integrative autonomic control. Dashed green lines indicate parasympathetic efferent pathways; only pelvic and vagal nerves are shown and, as to the vagus, only its cardiac innervation. For clarity, also efferent sympathetic pathways that leave the sympathetic chain to innervate the skin and the head are not shown; (A) celiac, (B) superior mesenteric, (C) inferior mesenteric ganglia. A spinal cord lesion occurring between T12 and L4, as in SCI_L individuals, may affect the autonomic control of organs innervated by the pelvic nerve and by efferent pathways from the two mesenteric ganglia (B) and (C). A higher lesion, between T5 and T11, as in SCI_H individuals, may also affect the autonomic control of organs innervated by efferent pathways from the celiac ganglion (A). In both cases, the autonomic control on the heart is preserved.

2.3. Power spectral analysis

Each tachogram was interpolated evenly at 5 Hz before spectral analysis. The Welch periodogram was estimated between 5.5×10^{-3} Hz and 0.512 Hz by employing 90% overlapped Hann windows of 180 s length. The resulting periodogram was smoothed with a broadband procedure, that averages contiguous spectral lines with a moving average filter whose order increases with the spectral frequency from 3 at the lowest frequency up to 17 at the highest frequency (Di Rienzo *et al* 1996). The power spectral density was integrated to obtain powers in the very-low frequency (VLF, 0.005–0.04 Hz), low-frequency (LF, 0.04–0.15 Hz) and high-frequency (HF, 0.15–0.40 Hz) bands, and to obtain the ratio between LF and HF powers, index of cardiac sympatho/vagal balance.

2.4. Fractal analysis

The self-similarity structure of heart rate variability was evaluated by the recently proposed temporal spectrum of scale coefficients (Castiglioni *et al* 2011a). This fractal method is an extension of the detrended fluctuation analysis algorithm, a popular tool for estimating a scale coefficient, α, closely related to the Hurst's exponent H (Peng *et al* 1995). In particular, $\alpha = H$ for stationary fractional Gaussian noises and $\alpha = H + 1$ for nonstationary fractional Brownian motions. This means that purely monofractal stochastic processes like white noises, '$1/f$' noises and Brownian motions have α values respectively equal to 0.5, to 1.0 and to 1.5.

To evaluate α of a time series $x(i)$ of N samples, with $i = 1,\ldots N$, first the cumulative summation $y(i)$ is obtained as:

$$y(i) = \sum_{j=1}^{i}(x(j) - \mu) \tag{1}$$

with μ the mean of the N values $x(i)$. Then $y(i)$ is split into consecutive, nonoverlapping blocks of n samples. A polynomial trend of order p is calculated in each of the N/n blocks of size n by least square fitting, and the piecewise function $y^p(n,i)$, with i from 1 to N, is obtained by connecting the trends of each block. The root mean square of the deviations of $y(i)$ from its local trend is evaluated as:

$$F_d(n) = \sqrt{\frac{1}{N}\sum_{i=1}^{N}(y(i) - y^p(n,i))^2} \tag{2}$$

For pure monofractal processes, $F_d(n)$ increases as the power α of n, i.e. $F_d(n) \propto n^\alpha$. Therefore, α can be estimated by evaluating (2) over a broad range of block sizes n and by calculating the slope of the regression line between $F_d(n)$ and n, both plotted in a logarithmic scale. However, it is commonly accepted that a single α coefficient does not provide a sufficiently precise description of real *R–R* intervals. For this reason, some authors modified the traditional detrended fluctuation analysis algorithm to obtain the coefficient α as a continuous function of the block size n (Echeverria *et al* 2003, Castiglioni *et al* 2009). According to our proposal, the detrended fluctuation function, $F_d(n)$, is estimated for a set of scales, n_k, with k between 1 and K, equispaced over the logarithmic scale. Then, a local scale exponent can be estimated at scales n_k, with k between 2 and $K - 1$, as the derivative of $\log F_d(n)$ versus $\log n$:

$$\alpha_B(n_k) = \frac{\log F_d(n_{k+1}) - \log F_d(n_{k-1})}{\log n_{k+1} - \log n_{k-1}} \tag{3}$$

The $\alpha_B(n)$ function is defined over the 'beat' domain n. This makes it difficult comparing conditions with different mean heart rates, because the same block size n may correspond to different time scales. In this case, it is useful to map $\alpha_B(n)$ into the time domain with the following transformation:

$$\alpha(\tau_k) = \alpha_B(n_k) \quad \text{with } \tau_k = n_k \times \mu \tag{4}$$

where μ is the mean *R–R* interval, in seconds. By linearly interpolating $\alpha(\tau_k)$ over the time scale, the 'emporal spectrum of scale coefficients', $\alpha(\tau)$, is finally obtained.

The shortest temporal scale τ that can be reasonably estimated without substantial estimation bias depends on the order p of the fitting polynomial in (2). The block size n should be greater than $p + 1$, or the fitting polynomial would pass exactly through all the n points resulting in a null detrended fluctuation function; however, it should also be sufficiently greater than $p + 1$, to avoid overfitting the data. In this analysis, we set $p = 1$ (i.e. the detrending

polynomial is a straight line) and $\tau = 5$ as the shortest temporal scale. On average, time scales of 5 s correspond to block sizes n of about 6 heart beats and, as shown with synthesized data (Kantelhardt *et al* 2001), this block size is sufficiently large to avoid estimation bias.

The longest temporal scale that can be assessed depends on the length of the time series. In a previous study we empirically quantified errors in estimating $\alpha(\tau)$ at the larger scales by analyzing a long-term ECG Holter recording during normal daily activities (Castiglioni *et al* 2011b). This previous study indicated that given a *R–R* interval series of 10 min, $\alpha(\tau)$ can be estimated without bias up to $\tau = 80$ s. In this study, we are considering a different experimental condition (subjects sitting at rest) and it cannot be excluded that this more stable condition may allow extending the estimation at larger τ values. In appendix, we performed an empirical evaluation of estimation bias on long-term ECG recordings obtained in 10 individuals with general characteristics similar to those of our volunteers, in sitting position. Results of the empirical simulation show that when the length of the recording is 10 min, errors associated with estimation bias are sufficiently small up to $\tau = 120$ s to be considered acceptable for this study. Therefore, we extended our estimation of the temporal spectrum of scale coefficients for τ between 5 and 120 s.

2.5. Statistics

Power spectra were log-transformed before statistical analysis to reduce the skewness of the distributions (Castiglioni *et al* 1999) and to apply parametric statistics based on Student's *t* distribution. The $\alpha(\tau)$ spectra were not transformed since scale coefficients follow a normal distribution (Castiglioni *et al* 2011b). Differences between controls and each of the two subgroups of paraplegic subjects were quantified by calculating the Student's *t* function at each spectral frequency f and at each temporal scale τ.

3. Results

The average *R–R* interval was 864 (172) ms in the AB group, values as mean (standard deviation). The corresponding average *R–R* interval in the SCI_L group was similar, being 853 (129) ms, with $p = 0.80$ for the difference versus AB (unpaired *t*-test). The *R–R* interval of SCI_H individuals was 778 (172) ms, slightly lower than in the AB group, although with a weak statistical significance ($p = 0.08$).

Figure 2 compares the power spectra of spinal cord injured individuals with the power spectra of controls. Paraplegic subjects with the lower lesion level, between T12 and L4, and controls had very similar power spectra (left panels). In particular, values of Student's *t* function evaluated for their two-tail difference were consistently lower than the 5% significance threshold over the whole range of frequencies. Also powers in VLF, LF and HF bands do not reveal differences between AB and SCI_L groups (table 1).

Figure 3 compares the $\alpha(\tau)$ fractal spectrum of controls with $\alpha(\tau)$ of each group of paraplegic individuals. The shape of AB and SCI_L fractal spectra are remarkably similar (left panels). Both are characterized (1) by an absolute maximum at the shortest scale ($\tau = 5$ s), with α slightly greater than 1 ($\alpha = 1.12$ in AB and $=1.14$ in SCI_L); (2) a minimum at $\tau = 17$ s; (3) a maximum at $\tau = 33$ s; and (4) the same value, $\alpha = 0.78$, at the largest scale, $\tau = 120$ s. However, the average fractal spectrum tends to be greater in the SCI_L group for scales between 5 and 120 s. The corresponding Student's *t* function points out that the larger differences between the distributions of AB and SCI_L spectra occur at scale τ between 12 and 48 s, where the significance level is lower than 5%. At $\tau = 33$ s, α is 0.83 in the AB group, and 0.95 in the SCI_L group.

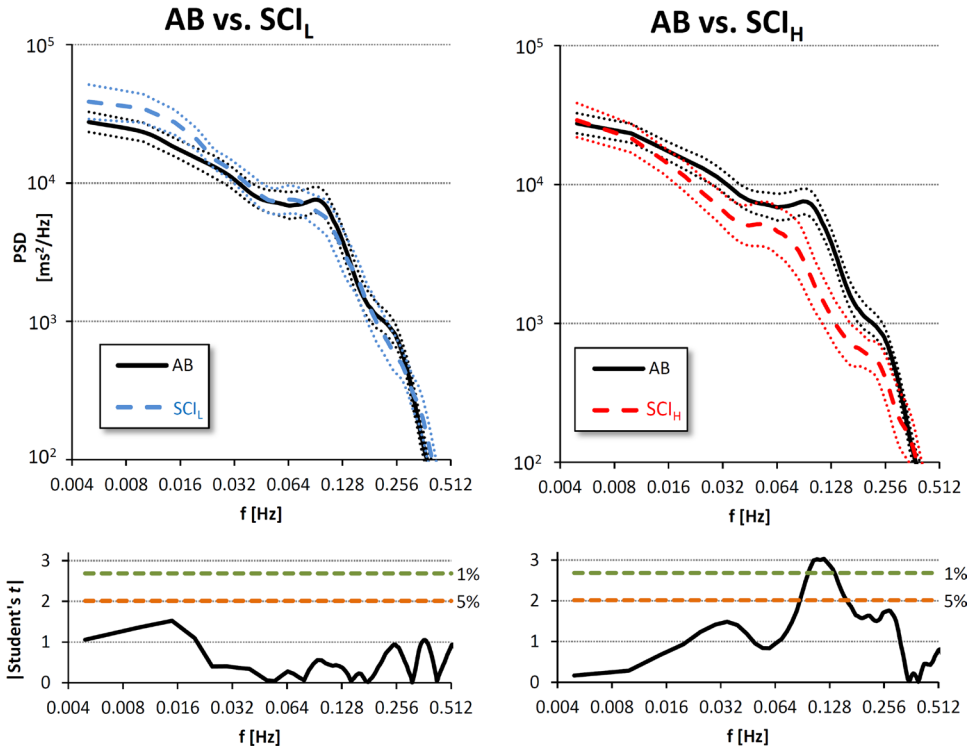

Figure 2. Power spectral analysis. (left) Comparison between AB and SCI_L groups; (right) comparison between AB and SCI_H groups. The upper panels show the power spectral densities as mean $\pm$ standard error of the mean; the lower panels shows the modulus of the student's t function associated with the difference between AB and SCI_L groups (left) or SCI_H groups (right) for each spectral line. The dashed horizontal lines mark the thresholds associated with 5% and 1% two-tail limits of the distribution. They correspond to the t values where the area under the curve of the probability distribution at $N_{AB} + N_{SCI} - 2$ degrees of freedom (with $N_{AB} = 34$ the size of the AB group, $N_{SCI} = 14$ the size of SCI_L or of SCI_H group) reach 0.975 and 0.995 respectively.

Table 1. Powers in the VLF, LF and HF bands and LF/HF powers ratio in the AB, SCI_L and SCI_H groups, as mean and standard deviation (values after log transformation).

	AB	SCI_L		SCI_H	
	M (SD)	M (SD)	p versus AB	M (SD)	p versus AB
VLF ($\log_{10}$ ms^2)	2.83 (0.40)	2.94 (0.34)	0.34	2.74 (0.40)	0.48
LF ($\log_{10}$ ms^2)	2.84 (0.51)	2.81 (0.41)	0.84	2.50 (0.64)	0.06
HF ($\log_{10}$ ms^2)	2.28 (0.45)	2.25 (0.46)	0.83	2.03 (0.52)	0.11
LF/HF ($\log_{10}$)	0.56 (0.27)	0.56 (0.22)	0.99	0.47 (0.46)	0.43

By contrast, the comparison between AB and SCI_H groups reveal a lower spectral power around the LF band in paraplegic subjects (figure 2, right panels), with the Student's t function crossing the 5% significance threshold between 0.09 Hz and 0.16 Hz. Consequently, the LF power tends to be lower in SCI_H than in AB individuals (table 1).

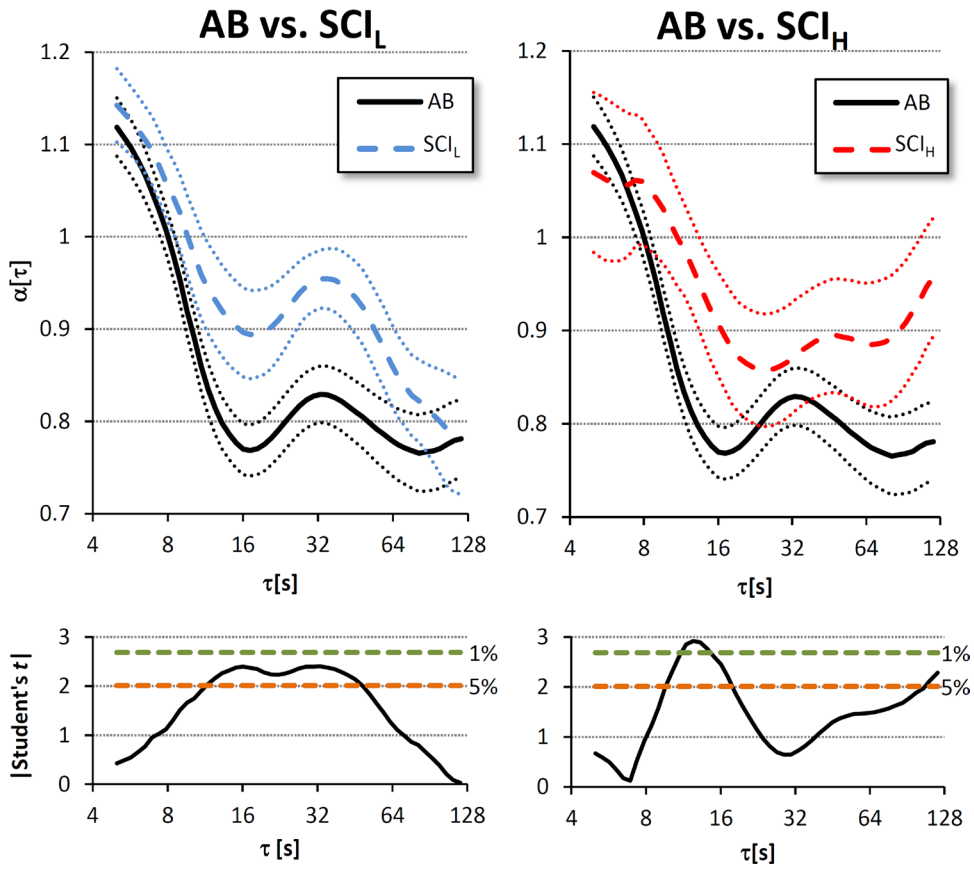

Figure 3. Fractal analysis. (left) Comparison between AB and SCI_L groups; (right) comparison between AB and SCI_H groups. Upper panels: temporal spectra of scale coefficients as mean $\pm$ standard error of the mean. Lower panels: modulus of the student's t function associated with the difference between AB and SCI_L groups (left) or SCI_H groups (right) at each scale τ.

Also the comparison between AB and SCI_H fractal spectra (figure 3, right panels) reveal differences between these two groups. As in SCI_L individuals, the fractal spectrum of the SCI_H group has its maximum at the shortest scales ($\alpha = 1.07$ at $\tau = 5$ s) and tends to be greater than in controls at scales larger than 10 s. However, unlike the SCI_L fractal spectrum, $\alpha(\tau)$ of SCI_H individuals does not show the relative maximum at $\tau = 33$ s that also characterizes the AB group. In addition, while the $\alpha(\tau)$ functions of SCI_L and AB groups start to converge at τ larger than 32 s, reaching the same value at $\tau = 120$ s, the $\alpha(\tau)$ functions of SCI_H and AB groups start to diverge at τ larger than 32 s, and at $\tau = 120$ s the self-similarity coefficient of the SCI_H group reaches an α value substantially greater than in controls ($\alpha = 0.96$, $p < 5\%$).

4. Discussion

This work demonstrated that methods of fractal analysis may reveal changes in heart rate variability likely associated to an altered integrative control of circulation, since they occur in individuals with a spinal cord lesion that leaves intact the autonomic cardiac efferent pathways

and the cardiac baroreflex loop. This work also reports, for the first time to our knowledge, alterations in specific components of heart rate fractal dynamics even in absence of any noticeable alteration in the power spectrum of heart rate variability. This was the case of SCI_L individuals, where the spinal lesion compromises the vegetative control of the lower districts only. In SCI_H individuals, with higher lesion levels but still with intact cardiac autonomic outflows, both power and fractal spectra were altered but at different frequencies (or temporal scales), thus providing complementary information, potentially helpful for better understanding the autonomic cardiovascular control.

The power spectrum allows a precise quantification of the amplitude of heart rate fluctuations at different frequencies separately. The faster oscillation of interest is the respiratory sinus arrhythmia, mainly due to modulations on the sinus node of the efferent vagal activity (Task Force of the European Society of Cardiology and the North American Society of Pacing and Electrophysiology 1996). Such fast modulations may have a central origin from cardiorespiratory centers and/or a baroreflex origin in response to blood pressure oscillations induced mechanically by respiration. Our results are in line with these hypotheses. In fact, direct autonomic efferent pathways from higher neural centers and the cardiac baroreflex loop are intact when the spinal lesion is below the fourth thoracic vertebra, and consequently we did not find differences in the power of respiratory oscillations between AB controls and SCI_L or SCI_H individuals.

A second oscillatory component occurs at a lower frequency in both heart rate and blood pressure. It is the so-called 10 s rhythm, or Mayer's wave. In our study we found a reduction in the heart-rate power spectrum of SCI_H individuals only, that regards frequencies between 0.09 Hz and 0.16 Hz. Therefore, the power reduction includes the Mayer waves, responsible for the clear spectral peak at 0.1 Hz in the AB spectrum. Interestingly, a possible explanation for the '0.1 Hz oscillation' in blood pressure is the hypothesis of 'baroreflex resonance'. Accordingly, the baroreceptors sense blood pressure changes and generate autonomic modulations on the vasculature, which undergo a $-180°$ phase shift at around 0.1 Hz because of the delay in neural modulations of peripheral resistances. This phase shift results in a positive feedback sustaining the oscillation (Julien 2006). The baroreflex arc connecting the baroreceptors with the heart is intact in our paraplegic volunteers, and therefore the lack of power around 0.1 Hz in SCI_H and not in SCI_L individuals would indicate that the resonant oscillation of blood pressure is lost in the SCI_H group only. This means that when the spinal lesion is enough low so that autonomic modulations can reach the splanchnic district from the medulla, the baroreflex control of vascular resistances is sufficiently preserved to be able to generate a resonance oscillation in blood pressure. Accordingly with this hypothesis, we previously showed that the LF peak of blood pressure and heart rate spectra was partially impaired in a heterogeneous group of paraplegic subjects with lesion below the fourth thoracic vertebra (Castiglioni *et al* 2007). The present study in addition clarifies that an intact autonomic control of the vascular splanchnic district is sufficient for producing the LF spectral peak, because SCI_L and AB spectral powers were similar around 0.1 Hz. Actually, the only difference in power spectra we found comparing these two human models of impaired autonomic integrative control with AB individuals, is the lower LF power for the SCI_H group only.

Unlike the power spectrum, the temporal spectrum of scale coefficients does not describe the amplitude of oscillations but the structure of self-similarity, at different scales separately. The shape of the $\alpha(\tau)$ function in AB controls of this study is remarkably similar to the heart-rate $\alpha(\tau)$ reported previously in groups of healthy volunteers sitting at rest (Castiglioni *et al* 2009, 2015). Common features are the highest value occurring at the shortest scale, and a relative maximum at τ around 30 s. The relative maximum cannot be an artifact induced by the 0.1 Hz oscillation, because the time scale is larger than the periodicity of the Mayer's

wave, and because the relative maximum is absent in diastolic blood pressure (Castiglioni *et al* 2015) where, by contrast, the LF spectral peak is particularly evident. It is conceivable that the relative maximum at τ around 30 s derives from a properly weighted mixture of the different contributions to $\alpha(\tau)$ provided by cardiac vagal and cardiac sympathetic outflows. Actually, pharmacological autonomic blockade in humans showed that at scales shorter than 60 s the two autonomic branches contribute with rather different components: the vagal outflow contributes with 'white noise' components, while the sympathetic outflow contributes with 'Brownian motion' components (Castiglioni *et al* 2011a). Our results would therefore suggest that the balance between sympathetic and vagal contributions to $\alpha(\tau)$ is substantially preserved in the SCI_L group, so that the profile of $\alpha(\tau)$ shows the same morphology as in controls.

In addition, results in the SCI_L group demonstrate that alterations in the autonomic control of the lower vascular districts, even if unable to substantially alter the power of heart-rate oscillations, may noticeably alter the structure of heart-rate self similarity, increasing specific α coefficients so that the heart rate dynamics is closer to a '$1/f$' noise at scales of tens of seconds. The loss of the autonomic regulation from higher neural centers regards the lower vascular districts only in the SCI_L group. Therefore, we might hypothesize that loss of regulation in the lower vascular beds only causes a compensatory increase of the regulative activity in the intact higher vascular districts. The increased vascular sympathetic activity might result in an enhanced fractal component of heart rate variability associated with the cardiac sympathetic outflow. Making use of autonomic blockade (Castiglioni *et al* 2011a) we previously showed that (1) the heart-rate fractal spectrum is the superimposition of two components, one due to the cardiac vagal outflow and one due to the cardiac sympathetic outflow; and that (2) the sympathetic fractal component increases from white-noise coefficients at scales larger than 60 s, up to Brownian- motion coefficients at the shorter scales. Therefore, an increase of the relative weight of the sympathetic fractal component might result in larger coefficients at scales shorter than 60 s, in line with the present observation of larger alpha coefficients in SCI_L at scales shorter than 48 s. However, when both the cardiac vagal and cardiac sympathetic outflows are present, as in our SCI_L group, vagal heart-rate modulations dominate the shorter scales. This might explain why the increase in scale coefficients is no more statistically significant at scales shorter than 12 s.

Results in the SCI_H group indicate that when the lesion is sufficiently high to involve the autonomic information travelling through greater, lesser and lumbar splanchnic nerves, thus affecting the autonomic control of all the splanchnic districts (see figure 1), the fractal structure of heart rate dynamics is so importantly altered that the relative maximum, characterizing both the AB and the SCI_L groups, disappear completely. The effect of the spinal lesion is to basically increase the value of scale coefficients, as in SCI_L individuals. However, a different range of temporal scales is affected in the SCI_H group. In particular, differences between SCI_H and AB individuals are remarkable at the longest scale considered in this work ($\tau = 120$ s): at this scale, α is close to the level that characterize a '$1/f$' process. It is worth to note that information provided by the temporal spectrum of scale coefficients is complementary to information provided by power spectral analysis. In fact, the difference between AB and SCI_H groups in the scale coefficient at the longest scale is not associated with any difference in the power of spectral lines in the very low frequency band.

4.1. Study limitations

The interpretation of results should consider some limitations that are typical of comparisons between AB and paraplegic individuals. First, the level of physical activity may be expected to be lower in paraplegic individuals than in AB controls, and a sedentary lifestyle might

influence the overall autonomic control. However, we enrolled paraplegic individuals that regularly practice sport activities. Since paraplegic individuals have similar training adaptation of the heart as able bodied subjects, apart from some differences in LV dimension and function (Maggioni *et al* 2012), it is likely that sedentary did not influence our results importantly. Second, unlike AB controls, some paraplegic individuals were taking antibiotics for urinary tract infections (18%) or drugs to relieve muscle spasms (14%). In any case, the prevalence of such pharmacological treatments was very similar in SCI_H and SCI_L groups, as indicated in methods. Therefore, these treatments should not have influenced the different way in which a spinal cord lesion affects $\alpha(\tau)$ in SCI_H and SCI_L individuals.

In conclusion, we expect that a spinal cord lesion, that disconnect the vascular beds below the lesion level from the flow of autonomic information passing through the medulla, may alter the 'overall complexity' of the cardiovascular system, because it would decrease the number of independent vascular subsystems that interact directly with the autonomic nervous system, and that exchange information with higher neural centers through neural pathways in the spinal cord. Assuming that the cardiovascular system behaves as a 'complex dynamical system', its 'complexity' may generate variability components of the outputs variable not characterized by an intrinsic time scale. This would imply that changes in complexity are more likely associated with changes in the heart rate fractal characteristics rather than with changes in heart rate spectral powers. In line with our hypothesis, we actually showed that a proper quantification of the fractal components of heart rate variability can reveal the alterations in the integrative autonomic control expected to occur in paraplegic individuals, even if the population selected for this study does not show any relevant sign of dysautonomia. Moreover, the fractal approach we followed appears more sensitive than power spectral analysis, being able to identify significant alterations even in the SCI_L group, where the power spectrum was unable to detect any difference with AB controls. Our results therefore suggests that fractal analysis of heart rate variability may be a valid tool for characterizing the residual integrative autonomic control in paraplegic individuals, an aspect that cannot be quantified by current neurological tests; or for detecting the first, faded signs of subclinical autonomic dysfunction, in populations at risks, as hypertensive or diabetic individuals. AQ3

Appendix. Estimation bias due to the use of short data segments

The length of the time series limits the longest temporal scale τ at which $\alpha(\tau)$ can be estimated without substantial errors. The scale τ is proportional to the block size n in equation (2). If n is too large compared to the length of the series, N, then the number of independent segments for calculating the deviations from the local trend, N/n, could be too low, affecting the quality of the estimate. Estimation errors can be random or systematic. Random errors increase the variance of the estimate; their effect can be reduced by increasing the size of the studied populations. By contrast, systematic errors cause estimation bias that may alter the shape of $\alpha(\tau)$ group averages, and that, unlike errors due to estimation variance, cannot be reduced by increasing the size of the studied population. For this reason, we empirically evaluated whether the range of temporal scales τ we considered in our study (from 5 to 120 s) is or not associated with an acceptable level of estimation bias when the length of the *R–R* interval series is 10 min, as in our recordings.

For this evaluation, we should consider reference ECG recordings much longer than 10 min. Therefore, from our database we selected an additional set of ten ECG recordings obtained for at least 1 h and half in 10 healthy normotensive volunteers (2 females and 8 males) in sitting position. Their age was 37.7 (9.1) years and body mass index 24.6 (2.9) kg m^{-2}, mean (SD).

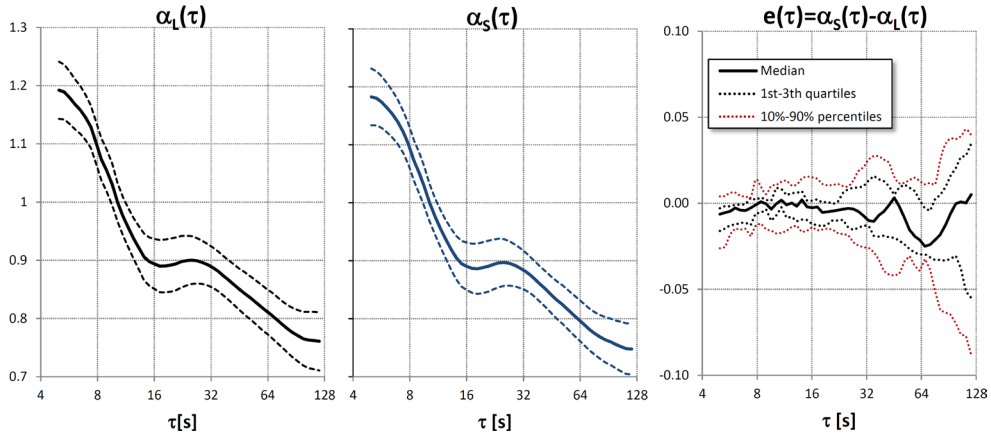

Figure A1. Heart rate variability fractal analysis with data windows of long and short duration. Left and central panels: self-similarity spectrum of scale coefficients evaluated over a single data window of 5400 s length, $\alpha_L(\tau)$, or over 9 consecutive data windows of 600 s length, $\alpha_S(\tau)$: mean ± standard error of the mean over a group of 10 healthy volunteers. Right panel: corresponding estimation error.

In each recording we selected a reference data segment of 5400 s. We calculated the temporal spectrum of scale coefficients for $5 \leqslant \tau \leqslant 120$ s, over a single data window covering the whole data segment, as the reference 'long-window' estimate, $\alpha_L(\tau)$. We may assume a null estimation bias for $\alpha_L(\tau)$ even at the longest scale ($\tau = 120$ s) because the number of independent segments for estimating $F_d(n)$ is ⩾45 at all the scales. Then the 5400 s long window was split into 9 consecutive, non overlapping windows, of 600 s length. A temporal spectrum of scale coefficient was calculated in each of these shorter windows, $\alpha^i(\tau)$ with $i = 1,\ldots,9$. The 9 $\alpha^i(\tau)$ fractal spectra were averaged at each temporal scale, obtaining the 'short-window' estimate, $\alpha_S(\tau)$. The averaging procedure does not reduce systematic errors and therefore any estimation bias in $\alpha^i(\tau)$ also affects $\alpha_S(\tau)$. The $\alpha_L(\tau)$ and $\alpha_S(\tau)$ can be directly compared because both evaluated at the same scales τ considering the same original data segment of 5400 s. Systematic estimation errors were quantified as: $e(\tau) = \alpha_S(\tau) - \alpha_L(\tau)$.

Figure A1 (left and central panels) shows the average over the group of $\alpha_L(\tau)$ and $\alpha_L(\tau)$. Differences between estimates are hardly noticeable. Systematic estimation errors are shown in the right panel of figure A1, as median, quartiles and percentiles of the $e(\tau)$ distribution over the group. Errors suggest that evaluations on 10 min data segments tend to underestimate $\alpha_L(\tau)$ at the longer scales. However, the magnitude of the error appears so small that can be considered negligible for the present study.

AQ4 ## References

Bak P, Tang C and Wiesenfeld K 1987 Self-organized criticality: an explanation of the 1/*f* noise *Phys. Rev. Lett.* **59** 381–4

Castiglioni P, Brambilla V, Brambilla L, Gualerzi M, Lazzeroni D and Coruzzi P 2015 The fractal structure of cardiovascular beat-to-beat series described over a broad range of scales: differences between blood pressure and heart rate, and the effect of gender *Conf. Proc., IEEE Engineering in Medicine and Biology Society* vol 2015 pp 290–3

Castiglioni P, Di Rienzo M, Veicsteinas A, Parati G and Merati G 2007 Mechanisms of blood pressure and heart rate variability: an insight from low-level paraplegia *Am. J. Physiol. Regul. Integr. Comput. Physiol.* **292** R1502–9

Castiglioni P, Parati G, Civijian A, Quintin L and Di Rienzo M 2009 Local scale exponents of blood pressure and heart rate variability by detrended fluctuation analysis: effects of posture, exercise, and aging *IEEE Trans. Biomed. Eng.* **56** 675–84

Castiglioni P, Parati G, Di Rienzo M, Carabalona R, Cividjian A and Quintin L 2011a Scale exponents of blood pressure and heart rate during autonomic blockade as assessed by detrended fluctuation analysis *J. Physiol.* **589** 355–69

Castiglioni P, Parati G, Lombardi C, Quintin L and Di Rienzo M 2011b Assessing the fractal structure of heart rate by the temporal spectrum of scale exponents: a new approach for detrended fluctuation analysis of heart rate variability *Biomed. Technol.* **56** 175–83

Castiglioni P, Parati G, Omboni S, Mancia G, Imholz B P, Wesseling K H and Di Rienzo M 1999 Broad-band spectral analysis of 24 h continuous finger blood pressure: comparison with intra-arterial recordings *Clin. Sci.* **97** 129–39

Di Rienzo M, Castiglioni P, Parati G, Mancia G and Pedotti A 1996 Effects of sino-aortic denervation on spectral characteristics of blood pressure and pulse interval variability: a wide-band approach *Med. Biol. Eng. Comput.* **34** 133–41

Echeverria J C, Woolfson M S, Crowe J A, Hayes-Gill B R, Croaker G D and Vyas H 2003 Interpretation of heart rate variability via detrended fluctuation analysis and alphabeta filter *Chaos* **13** 467–75

Huikuri H V, Perkiomaki J S, Maestri R and Pinna G D 2009 Clinical impact of evaluation of cardiovascular control by novel methods of heart rate dynamics *Phil. Trans.* A **367** 1223–38

Julien C 2006 The enigma of Mayer waves: facts and models *Cardiovasc. Res.* **70** 12–21

Kantelhardt J W, Koscielny-Bunde E, Rego H H A, Havlin S and Bunde A 2001 Detecting long-range correlations with detrended fluctuation analysis *Physica* A **295** 441–54

Kobayashi M and Musha T 1982 1/*f* fluctuation of heartbeat period *IEEE Trans. Biomed. Eng.* **29** 456–7

Maggioni M A, Ferratini M, Pezzano A, Heyman J E, Agnello L, Veicsteinas A and Merati G 2012 Heart adaptations to long-term aerobic training in paraplegic subjects: an echocardiographic study *Spinal Cord* **50** 538–42

Peng C K, Havlin S, Hausdorff J M, Mietus J E, Stanley H E and Goldberger A L 1995 Fractal mechanisms and heart rate dynamics. Long-range correlations and their breakdown with disease *J. Electrocardiol.* **28** 59–65

Perkiomaki J S 2011 Heart rate variability and non-linear dynamics in risk stratification *Frontiers Physiol.* **2** 81

Sassi R, Cerutti S, Lombardi F, Malik M, Huikuri H V, Peng C K, Schmidt G and Yamamoto Y 2015 Advances in heart rate variability signal analysis: joint position statement by the e-cardiology ESC Working Group and the European Heart Rhythm Association co-endorsed by the Asia Pacific Heart Rhythm Society *Europace* **17** 1341–53

Task Force of the European Society of Cardiology and the North American Society of Pacing and Electrophysiology 1996 Heart rate variability. Standards of measurement, physiological interpretation, and clinical use *Eur. Heart J.* **17** 354–81

West G B, Brown J H and Enquist B J 1997 A general model for the origin of allometric scaling laws in biology *Science* **276** 122–6